Journal of Sound and Vibration (1997) **202**(4), 461–476

ACTIVE CONTROL OF SOUND FIELDS FROM A COMPOSITE PLATE USING THE ANISOTROPY AND SHAPE OF DISTRIBUTED PVDF ACTUATORS

S. J. Kim and K. W. Yoon

Department of Aerospace Engineering, Seoul National University, Seoul 151-742, *Republic of Korea*

(*Received* 7 *August* 1996, *and in final form* 6 *November* 1996)

Compared to piezoceramic material, polyvinylidene fluoride polymer has anisotropic electromechanical material properties. Using the fact that the anisotropy and shape of distributed piezopolymer actuators have coupling effects with the vibration modes of structures, studies on the design of distributed piezopolymer actuators are performed in order to improve the effectiveness of active control of the sound fields radiated from composite structures. The sound fields induced by the complicated dynamic behaviors of a composite structure was analyzed using coupled finite element and boundary element methods. Active control of sound fields is attempted through minimization of the radiated sound power from a plate. Some numerical results of sound control problems are presented with actuators of various shapes and lamination angles. The results indicate that the anisotropy and shape of distributed piezopolymer actuators are promising factors in the design of distributed piezoelectric actuators for controlling acoustic radiation from structures.

1. INTRODUCTION

Sound radiation from vibrating structures is an important problem in numerous engineering applications. One of the representative examples is sound radiation and transmission by aircraft fuselage panels. During recent decades, considerable efforts have been devoted to active control techniques to reduce low frequency sound radiated from vibrating structures. For structurally radiated or transmitted noise, the sound field is directly coupled to the structural motion. Therefore it is efficient to apply the control force inputs to the vibrating structure directly for the minimization of radiated sound fields [1, 2].

Fiber reinforced composite, which has anisotropic material properties, presents various distinguished features compared to conventional materials. It has been widely used as a primary material in industrial fields. In recent years, the acoustical characteristics of composite structures have been investigated [3, 4].

As a result of rapid advances in smart structures, the research thrust today is towards using the piezoelectric materials as distributed sensors or actuators in control applications. These smart materials have also been employed as actuators or sensors in active structural acoustic control problems. In particular, piezoelectric materials have received a

0022–460X/97/190461 + 16 $25.00/0/sv960857

considerable amount of attention in vibration control due to their availability. Polyvinylidene fluoride polymer (PVDF) is characterized by good properties such as flexibility, ruggedness, softness and lower weight. However, it is not as powerful as piezoceramic material (PZT). Hence, compared to PZT, PVDF has usually been used as a sensor rather than an actuator. However, PVDF has anisotropic electromechanical properties; that is, the piezo strain constants d_{31} and d_{32} of PVDF differ by an order of magnitude. This anisotropic characteristic of PVDF is an advantageous property for actuators and sensors in control applications [5].

Analyses on active structural acoustic control by using piezoelectric materials as actuators and sensors have been carried out extensively in recent years. Fuller *et al*. [6] used one collocated PZT actuator for the control experiment of sound fields from an isotropic plate. In this analysis, the piezoelectric actuator provided global attenuation of sound radiation from structural elements. In another experimental analysis [7], it was said that for the improvement of sound attenuation, the number of collocated piezoelectric actuators needs to be increased, and that the position of the collocated actuator is important in sound control. Koshigoe *et al*. [8] applied a simple PZT actuator to the control of sound transmission into a cavity, using a simple PZT actuator in their numerical investigation. PVDF film has been generally used as a sensor. Therefore, the effects of its shape have usually been discussed in connection with distributed sensors. Clark *et al*. [9] implemented the PVDF sensor as a narrow strip bonded horizontally and vertically on an isotropic plate for sound control. Then Clark *et al*. applied the PVDF sensor to the control of sound from an isotropic beam structure, through designing the shape of a PVDF modal sensor [10].

The main focus of current research is to investigate the effects of the anisotropic characteristics and the shape of distributed PVDF actuators in active control of sound radiation induced by the vibration of a composite plate structure. The distributed PVDF actuator attached to the surface of a composite has its own ply angle, similar to each lamina in a composite plate. Sound fields from an integrated structure are highly influenced by the interaction of vibration modes of the structure. Therefore the shape and directional characteristics of a PVDF actuator can be utilized in order to design an efficient actuator by considering the relationship between the vibration modes of the structure and the control effects due to the PVDF actuator.

The vibration of a composite plate and the sound radiation from the plate are analyzed by using the coupled finite element and boundary element methods. The finite element model of the composite plate is based on the first order shear deformation theory. Classical plate theory has usually been applied in the analysis of sound fields from isotropic plates. However, it is well established that in the analysis of composite plates a theory that includes shear deformation is required [11]. The finite element method (FEM) is efficient for simulating the dynamic behavior of composite plates with anisotropic characteristics, which is a formidable task by an analytical approach. The acoustic field is to be analyzed through the boundary element method (BEM) based on the Rayleigh integral equation.

For the global reduction of acoustic noise from the structure, the sound power is selected as the objective function in the control scheme. Some numerical calculations are carried out on sound fields from elastic plates. In order to investigate the effects of the anisotropy and shape of distributed piezopolymer actuators, various kinds of distributed PVDF actuators are applied in sound control simulation for isotropic and anisotropic plates. The PVDF actuators applied are different from each other in their shapes and laminate angles.

2. FORMULATION OF THE SYSTEM EQUATION

2.1. EQUATION OF THE STRUCTURAL SYSTEM

The structural system is an integrated plate (length a, width b and thickness h) containing fiber reinforced composite lamina and distributed piezoelectric actuators that are assumed to be perfectly bonded on the surface. The plate is supported in an infinite rigid baffle dividing the three-dimensional free space into two semi-infinite acoustic fields, as shown in Figure 1. Let the x–y plane coincide with the mid-plane of the plate, with the z-axis being normal to the mid-plane. The plate is a laminate consisting of a finite number of thin laminae, assumed to be perfectly bonded together. For a lamina, which is a fiber reinforced composite or piezoelectric material, its material axes are denoted as the 1-, 2- and 3-axes. The lamination angle of the ith lamina, θ_i, is defined as the angle from the x-axis to 1-axis in counterclockwise direction along the z-axis.

2.1.1. *Kinematics*

The displacement field $\{u_1, u_2, u_3\}$, based on the first order shear deformation theory [12], is given by

$$u_1(x, y, z, t) = u(x, y, t) + z\varphi_x(x, y, t), \qquad u_2(x, y, z, t) = v(x, y, t) + z\varphi_y(x, y, t),$$
$$u_3(x, y, z, t) = w(x, y, t), \tag{1}$$

where u, v and w are the displacements of a point (x, y) on the mid-plane, t is time and φ_x and φ_y are the rotations of the line element, initially normal to the mid-plane, about the y- and x-axes, respectively.

The infinitesimal strain relations give the strain, written as

$$\boldsymbol{\varepsilon} = [\varepsilon^0_{xx} + z\kappa_{xx} \quad \varepsilon^0_{yy} + z\kappa_{yy} \quad \varepsilon^0_{xy} + z\kappa_{xy} \quad \gamma_{xz} \quad \gamma_{yz}]^{\mathrm{T}}$$

where the membrane strain $\boldsymbol{\varepsilon}^0$, the bending strain $\boldsymbol{\kappa}$, and the shear strain $\boldsymbol{\gamma}$ are expressed as follows:

$$\boldsymbol{\varepsilon}^0 = [\varepsilon^0_{xx} \quad \varepsilon^0_{yy} \quad \varepsilon^0_{xy}]^{\mathrm{T}} = \left[\frac{\partial u}{\partial x} \quad \frac{\partial v}{\partial y} \quad \frac{\partial u}{\partial y} + \frac{\partial v}{\partial x}\right]^{\mathrm{T}},$$

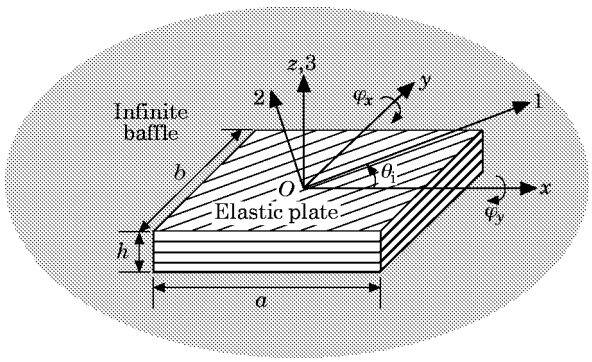

Figure 1. An integrated composite plate structure supported on an infinite rigid baffle.

$$\boldsymbol{\kappa} = [\kappa_{xx} \quad \kappa_{yy} \quad \kappa_{xy}]^{\mathrm{T}} = \left[\frac{\partial \varphi_x}{\partial x} \quad \frac{\partial \varphi_y}{\partial y} \quad \frac{\partial \varphi_x}{\partial y} + \frac{\partial \varphi_y}{\partial x}\right]^{\mathrm{T}},$$

$$\boldsymbol{\gamma} = [\gamma_{xz} \quad \gamma_{yz}]^{\mathrm{T}} = \left[\frac{\partial w}{\partial x} + \varphi_x \quad \frac{\partial w}{\partial y} + \varphi_y\right]^{\mathrm{T}}. \tag{2}$$

2.1.2. *Constitutive relation*

Through co-ordinate transformation, the electromechanical constitutive relations for the ith lamina can be written using the x-, y- and z-axes, as

$$\boldsymbol{\sigma} = \mathbf{C}^i\boldsymbol{\varepsilon} - \mathbf{d}^i E^i, \tag{3}$$

where $\boldsymbol{\sigma}$ is the stress, $\mathbf{C}^i$ is the elastic stiffness matrix, E^i is the applied electric field intensity in the z-direction, and $\mathbf{d}^i$ is expressed in terms of the piezoelectric strain/charge coefficients d_{31} and d_{32} [13]:

$$\boldsymbol{\sigma} = \begin{Bmatrix} \sigma_{xx} \\ \sigma_{yy} \\ \sigma_{xy} \\ \tau_{xz} \\ \tau_{yz} \end{Bmatrix}, \qquad \mathbf{d}^i = \begin{Bmatrix} d^i_{xx} \\ d^i_{yy} \\ d^i_{xy} \\ d^i_{xz} \\ d^i_{yz} \end{Bmatrix} = \beta \begin{Bmatrix} (m_i^2 C^i_{11} + n_i^2 C^i_{12}) d^i_{31} + (n_i^2 C^i_{11} + m_i^2 C^i_{12}) d^i_{32} \\ (n_i^2 C^i_{11} + m_i^2 C^i_{12}) d^i_{31} + (m_i^2 C^i_{11} + n_i^2 C^i_{12}) d^i_{32} \\ m_i n_i (C^i_{11} - C^i_{12}) d^i_{31} - m_i n_i (C^i_{11} - C^i_{12}) d^i_{32} \\ 0 \\ 0 \end{Bmatrix},$$

where β is $+1$ for positive polling and -1 for negative polling, $m_i = \cos\theta_i$ and $n_i = \sin\theta_i$. Equation (3) is the general expression for the piezoelectric material, while for a composite lamina the piezoelectric strain/charge coefficients should be zero. For isotropic PZT, for which d_{31} and d_{32} are equal, d_{xx} is always equal to d_{yy} and d_{xy} is always zero, irrespective of the lamination angle. Thus isotropic PZT cannot generate a shear stress component, in case of anisotropic PVDF, for which d_{31} and d_{32} are different from each other, is able to generate a shear stress component. The shear stress component produced by a directionally attached anisotropic PVDF actuator can be taken advantage of effectively in the control of sound fields from a plate structure.

The laminate constitutive relations are expressed as

$$\mathbf{N} = \mathbf{A}\boldsymbol{\varepsilon}^0 + \mathbf{B}\boldsymbol{\kappa} - \bar{\mathbf{N}}, \qquad \mathbf{M} = \mathbf{B}\boldsymbol{\varepsilon}^0 + \mathbf{D}\boldsymbol{\kappa} - \bar{\mathbf{M}}, \qquad \mathbf{Q} = \mathbf{A}_{\mathrm{S}}\boldsymbol{\gamma}, \tag{4}$$

where $\mathbf{N}$ and $\mathbf{Q}$ are force resultant vectors and $\mathbf{M}$ is the moment resultant vector. These are expressed in terms of in-plane stresses, $\{\sigma_{xx} \ \sigma_{yy} \ \sigma_{xy}\}$, and transverse shear stresses, $\{\tau_{xz} \ \tau_{yz}\}$, as follows:

$$\{N_{ij}, M_{ij}\} = \int \{1, z\}\sigma_{ij}\,\mathrm{d}z, \qquad i, j = x, y,$$

$$\{Q_x, Q_y\} = \int \{\tau_{xz}, \tau_{yz}\}\,\mathrm{d}z,$$

and the elastic coefficient matrices obtained from elastic stiffness matrix:

$$\{A_{mn} \quad B_{mn} \quad D_{mn}\} = \int \{1 \quad z \quad z^2\} C^i_{mn}\,\mathrm{d}z, \qquad m, n = 1, 2, 6,$$

$$\{A_{S_{11}} \quad A_{S_{12}} \quad A_{S_{22}}\} = k \int \{C_{44}^i \quad C_{45}^i \quad C_{55}^i\}\, \mathrm{d}z,$$

where k is the transverse shear correction factor, which is 5/6 in this analysis.

In equation (4), $\bar{\mathbf{N}}$ and $\bar{\mathbf{M}}$ are the force and moment resultants due to the piezoelectric actuator:

$$\begin{Bmatrix} \bar{N}_{xx} \\ \bar{N}_{yy} \\ \bar{N}_{xy} \end{Bmatrix} = \begin{bmatrix} \hat{N}_{11} & \hat{N}_{12} & \cdots & \hat{N}_{1N_L} \\ \hat{N}_{21} & \hat{N}_{22} & \cdots & \hat{N}_{2N_L} \\ \hat{N}_{31} & \hat{N}_{32} & & \hat{N}_{3N_L} \end{bmatrix} \begin{Bmatrix} E^1 \\ E^2 \\ \vdots \\ E^{N_L} \end{Bmatrix},$$

$$\begin{Bmatrix} \bar{M}_{xx} \\ \bar{M}_{yy} \\ \bar{M}_{xy} \end{Bmatrix} = \begin{bmatrix} \hat{M}_{11} & \hat{M}_{12} & \cdots & \hat{M}_{1N_L} \\ \hat{M}_{21} & \hat{M}_{22} & \cdots & \hat{M}_{2N_L} \\ \hat{M}_{31} & \hat{M}_{32} & & \hat{M}_{3N_L} \end{bmatrix} \begin{Bmatrix} E_1 \\ E^2 \\ \vdots \\ E^{N_L} \end{Bmatrix}, \tag{5}$$

and

$$\begin{Bmatrix} \hat{N}_{1i} \\ \hat{N}_{2i} \\ \hat{N}_{3i} \end{Bmatrix} = \int_{z_{i-1}}^{z_i} \begin{Bmatrix} d_{xx}^i \\ d_{yy}^i \\ d_{xy}^i \end{Bmatrix} \mathrm{d}z, \qquad \begin{Bmatrix} \hat{M}_{1i} \\ \hat{M}_{2i} \\ \hat{M}_{3i} \end{Bmatrix} = \int_{z_{i-1}}^{z_i} z \begin{Bmatrix} d_{xx}^i \\ d_{yy}^i \\ d_{xy}^i \end{Bmatrix} \mathrm{d}z, \qquad i = 1, 2, \ldots, N_L,$$

and N_L is the total number of laminae in a laminate.

2.1.3. *Finite element formulation*

The variational statement of the equation of motion for an integrated structure is obtained using the Hamilton variational principle [14], which is expressed as

$$\tfrac{1}{2} \int_S \rho h \delta \dot{\mathbf{u}}^{\mathrm{T}} \dot{\mathbf{u}}\, \mathrm{d}S - \tfrac{1}{2} \int_S (\delta \boldsymbol{\varepsilon}^{0\mathrm{T}} \mathbf{N} + \delta \boldsymbol{\kappa}^{\mathrm{T}} \mathbf{M} + \delta \boldsymbol{\gamma}^{\mathrm{T}} \mathbf{Q})\, \mathrm{d}S + \int_S (q_{ext}(x, y, t)\delta w - p(x, y, t)\delta w)\, \mathrm{d}S = 0, \tag{6}$$

and leads to the final weak form in terms of the kinematic variables $\{u, v, w, \varphi_x, \varphi_y\}$. The external loads acting on the integrated structure are the distributed external load $q_{ext}(x, y, t)$ and the acoustic loading $p(x, y, t)$ due to the acoustic medium adjacent to the plate surface.

A four-node quadrilateral plate element is used in finite element discretization of the weak form. The displacement vector in a typical element e is interpolated using the Lagrangian interpolation function

$$\mathbf{u}^{\mathrm{e}} = \begin{Bmatrix} u^e \\ v^e \\ w^e \\ \varphi_x^e \\ \varphi_y^e \end{Bmatrix} = \sum_{n=1}^{4} \psi_n(\xi, n) \begin{Bmatrix} u_n \\ v_n \\ w_n \\ \varphi_{x_n} \\ \varphi_{y_n} \end{Bmatrix} \equiv \mathbf{H}^e \mathbf{q}^e, \tag{7}$$

where the Lagrangian interpolation function is expressed as

$$\psi_n(\xi, \eta) = \tfrac{1}{4}(1 + \xi_n\xi)(1 + \eta_n\eta), \qquad n = 1, 2, 3, 4, \tag{8}$$

in which (ξ_n, η_n) are the local co-ordinates of node n. In order to avoid the shear locking phenomenon, the mixed interpolation technique of Bathe *et al*. [15] is applied, so that the element matrices are calculated using a full four-point Gauss integration rule. Finally, the finite element equation of motion for the integrated structure is obtained as

$$\mathbf{M}\ddot{\mathbf{q}}(\mathbf{x}, t) + \mathbf{K}\mathbf{q}(\mathbf{x}, t) = \mathbf{f}_e(\mathbf{x}, t) + \mathbf{f}_p(\mathbf{x}, t) + \mathbf{f}_a(\mathbf{x}, t), \tag{9}$$

where $\mathbf{M}$ is the mass matrix, $\mathbf{K}$ is the stiffness matrix, $\mathbf{q}$ is the displacement vector, $\mathbf{f}_e$ is the external force vector, $\mathbf{f}_p$ is the force vector due to the piezoelectric actuator, and $\mathbf{f}_a$ is the force vector due to the sound pressure load. The force vector $\mathbf{f}_p$ due to the piezoelectric actuator is expressed as

$$\mathbf{f}_p = \left[\sum_{k=1}^{N^e} \int_{S^e} \{\mathbf{B}_M^{e\mathrm{T}}\hat{\mathbf{N}} + \mathbf{B}_B^{e\mathrm{T}}\hat{\mathbf{M}}\}\, \mathrm{d}S\right]\mathbf{E} \equiv \mathbf{\Gamma}\mathbf{E},$$

where $\mathbf{B}_M^e$ and $\mathbf{B}_B^e$ are the interpolation matrices of the in-plane and bending strain in typical element e, respectively.

With the mass and stiffness matrices, the natural frequencies and mode shapes are found using the subspace iteration method. Equation (9) is transformed using the modal co-ordinate transformation

$$\mathbf{q} = \mathbf{\Phi}\boldsymbol{\eta}, \tag{10}$$

where $\mathbf{\Phi}$ is the modal matrix and $\boldsymbol{\eta}$ is the modal co-ordinate vector. With the introduction of modal damping, the transformed modal co-ordinate equation can be written as

$$\{\mathbf{\Lambda} + \mathbf{\Xi} - \omega^2\mathbf{I}\}\boldsymbol{\eta} = \mathbf{\Phi}^{\mathrm{T}}(\mathbf{f}_e + \mathbf{f}_a + \mathbf{\Gamma}\mathbf{E}) \tag{11}$$

where

$$\mathbf{\Lambda} = \mathbf{\Phi}^{\mathrm{T}}\mathbf{K}\mathbf{\Phi}, \qquad \mathbf{\Xi} = \mathrm{diag}\,(2\zeta_i\omega_i\omega\},$$

$\mathbf{I}$ is the identity matrix, and the ζ_i are modal damping coefficients.

2.2. EQUATION OF THE ACOUSTICAL SYSTEM

2.2.1. *Governing equation*

The acoustic sound pressure at $\mathbf{x}$ in the acoustic domain induced by a vibrating plate in a baffle is governed by the Rayleigh equation, expressed as [16]

$$p(\mathbf{x}) = \int_{S(\mathbf{x}_s)} \left\{G(\mathbf{x}, \mathbf{x}_s)\, \frac{\partial p(\mathbf{x}_s)}{\partial n_s}\right\} \mathrm{d}S, \tag{12}$$

where k is the wavenumber, defined as $k = \omega/c$, with sound speed c and forcing frequency ω, S is the surface of the plate, $\mathbf{x}_s$ is the point on surface S, and $\mathbf{n}_s$ is the outward unit normal on S. The Green function in the semi-infinite domain in equation (12) is

$$G(\mathbf{x}, \mathbf{x}_s) = \frac{\mathrm{e}^{-\mathrm{i}k|\mathbf{x} - \mathbf{x}_s|}}{2\pi|\mathbf{x} - \mathbf{x}_s|}.$$

At the interface of the plate and the acoustic medium, the normal derivative of the pressure can be related to the outward normal component of velocity v_n on S as follows:

$$\partial p(\mathbf{x}_s)/\partial n_s = \rho_0 \ddot{u}_n(\mathbf{x}_s) = \mathrm{i}\omega\rho_0 v_n(\mathbf{x}_s). \tag{13}$$

2.2.2. *Boundary element formulation*

When equation (12) is discretized with equation (13) by using the boundary element technique, one obtains the matrix equation as

$$\mathbf{p} = \mathbf{G}\mathbf{v}_n, \tag{14}$$

where $\mathbf{p}$ is the vector containing the sound pressure at $\mathbf{x}$ and $\mathbf{v}_n$ is the normal velocity vector at a node on S. Matrix $\mathbf{G}$ in equation (14) is expressed as follows:

$$\mathbf{G} = \sum_{k=1}^{N^e} \left[\int_{S^e(\mathbf{x}_s)} \left\{ \mathrm{i}\omega\rho_0 \frac{\mathrm{e}^{-\mathrm{i}k|\mathbf{x}-\mathbf{x}_s^e|}}{2\pi|\mathbf{x}-\mathbf{x}_s^e|} \mathbf{H}^e \right\} \mathrm{d}S \right],$$

in which N^e is the number of elements. A four-node quadrilateral element with the same shape function as applied in equation (8) is used for the discretization, which promises compatibility with FEM through wet nodes.

When the pressure on S is to be calculated, $\mathbf{x}$ is collocated on a node of the element S^e. Then the integrand has an inverse distance singularity. This singular integrand should be treated carefully. In this analysis, the transformation method is used for singular integration [17]. The method divides the quadrilateral element domain into two triangular domains according to the collocation node. The triangular domains are then transformed into square domains, and so a Jacobian cancels out the singularity of the integrand. In the element calculation, a nine-point Gaussian quadrature rule is used for accuracy.

2.3. STRUCTURAL AND ACOUSTICAL COUPLING

The vector of normal velocities $\mathbf{v}_n$ in equation (14) is related to the vector of modal co-ordinates by the modal transformation and the transformation matrix $\mathbf{T}$, which transforms the nodal velocities in the finite element system into the normal velocity in the boundary element system:

$$\mathbf{v}_n = \mathbf{T}\dot{\mathbf{q}} = \mathrm{i}\omega\mathbf{T}\boldsymbol{\Phi}\boldsymbol{\eta}. \tag{15}$$

If the velocity $\mathbf{v}_n$ is eliminated from equation (14), the resulting equation is

$$\mathbf{p} = \mathrm{i}\omega\mathbf{G}\mathbf{T}\boldsymbol{\Phi}\boldsymbol{\eta}. \tag{16}$$

When the acoustic medium is a light fluid such as air, the effect of acoustic loading on the plate structure can be considered to be negligible. Acoustic sound is calculated by equation (16) and the modal co-ordinate vector is obtained by solving equation (11). The structural response of the composite plate is obtained from the modal transformation in equation (10).

2.4. MINIMIZATION OF RADIATED SOUND FIELDS

For the global minimization of sound fields induced by vibrating plates, sound power is selected as the control objective. The anisotropic PVDF films bonded on the surface of the plate are used as distributed actuators for sound suppression. The radiated sound

power is defined as the integral of the sound intensity over the surface of the vibrating plate:

$$\Pi = \tfrac{1}{2}\int_S \mathrm{Re}\,[p^*(\mathbf{x}_s)v_n(\mathbf{x}_s)]\,\mathrm{d}S, \tag{17}$$

where the superscript asterisk denotes a complex conjugate. One calculates the sound power by integrating the nodal values of the pressure and normal velocity, as

$$\Pi = \tfrac{1}{2}\,\mathrm{Re}\left[\mathbf{p}^{\mathrm{H}}\left\{\sum_{k=1}^{N^e}\int_{S^e}\mathbf{H}^{e\mathrm{T}}\mathbf{H}^e\,\mathrm{d}S\right\}\mathbf{v}_n\right] = \tfrac{1}{2}\mathrm{Re}\,[\mathbf{p}^{\mathrm{H}}\mathbf{R}\mathbf{v}_n],$$

where

$$\mathbf{R} = \sum_{k=1}^{N^e}\int_{S^e}\mathbf{H}^{e\mathrm{T}}\mathbf{H}^e\,\mathrm{d}S$$

and the superscript H denotes the Hermitian transpose of a matrix. Using equations (15) and (16), the suppression for the sound power can be written as

$$\Pi = \tfrac{1}{2}\,\mathrm{Re}\,[\omega^2\boldsymbol{\eta}^{\mathrm{H}}\boldsymbol{\Phi}^{\mathrm{T}}\mathbf{T}^{\mathrm{T}}\mathbf{G}\mathbf{R}\mathbf{T}\boldsymbol{\Phi}\boldsymbol{\eta}].$$

Eliminating the modal co-ordinate vector using equation (11), the sound power is written in terms of external loads and control inputs to PVDF actuators as

$$\Pi = \tfrac{1}{2}\mathrm{Re}\,[(\mathbf{f}_e + \boldsymbol{\Gamma}\mathbf{E})^{\mathrm{H}}\mathbf{Z}(\mathbf{f}_e + \boldsymbol{\Gamma}\mathbf{E})], \tag{18}$$

where

$$\mathbf{Z} = \omega^2\boldsymbol{\Phi}(\boldsymbol{\Lambda} + \boldsymbol{\Xi} - \omega^2\mathbf{I})^{-\mathrm{H}}\boldsymbol{\Phi}^{\mathrm{T}}\mathbf{T}^{\mathrm{T}}\mathbf{G}\mathbf{R}\mathbf{T}\boldsymbol{\Phi}(\boldsymbol{\Lambda} + \boldsymbol{\Xi} - \omega^2\mathbf{I})^{-1}\boldsymbol{\Phi}^{\mathrm{T}}.$$

The input electric field into the piezoelectric actuator is limited to less than about 10 volts per 1 μm. Therefore, the minimization problem for the sound power expressed in the form of equation (18) has the constraint that the control input should be less than the allowable limit for each PVDF actuator. The problem can be stated as follows:

$$\begin{array}{ll}\text{Minimize} & \tfrac{1}{2}\,\mathrm{Re}\,[(\mathbf{f}_e + \boldsymbol{\Gamma}\mathbf{E})^{\mathrm{H}}\mathbf{Z}(\mathbf{f}_e + \boldsymbol{\Gamma}\mathbf{E})] \\ \text{subject to} & \|E^k\| \leqslant l_k, \qquad k = 1, \ldots, n_A,\end{array}$$

where l_k is the allowable limit of the input for the kth actuator and n_A is the total number of actuators. This minimization problem is approached by applying the steepest descent method, so that the optimal control input can be obtained.

3. NUMERICAL RESULTS

In this section the results of numerical analyses are presented. These analyses involve the active control of sound radiation from a rectangular integrated composite plate supported on an infinite baffle and excited by vibrating forces. The acoustic medium is air, the density of which is 1·21 kg/m^3 and the wave velocity of which is 343 m/s. The coupled FEM–BEM analyses are carried out for the cases of an isotropic aluminum plate and an anisotropic composite plate with various boundary conditions. PVDF actuators used for control of the sound radiation and with different shapes and lamination angles to demonstrate various features of the actuators. In the analysis, 20 vibration modes of the

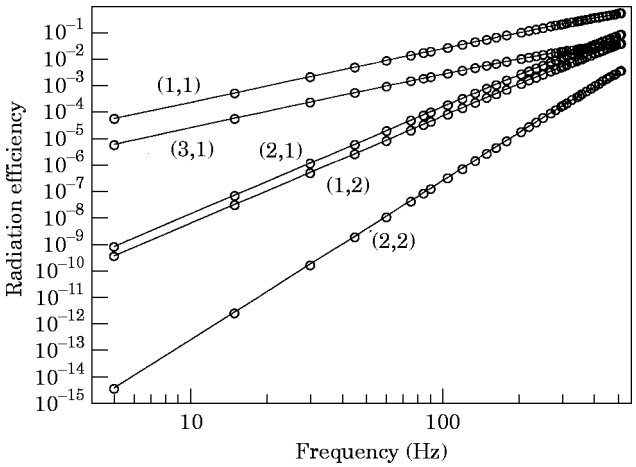

Figure 2. The modal radiation efficiencies of a simply supported isotropic plate. ——, Wallace [17]; ○, present result.

structure are used in modal transformation and a small amount of modal damping ($\zeta_i = 0{\cdot}01$) is used.

3.1. RADIATION EFFICIENCIES OF SIMPLY SUPPORTED ALUMINUM PLATE: VERIFICATION

In order to verify the coupled FEM–BEM analysis, the radiation efficiencies of lower vibration modes for a simply supported aluminum plate are analyzed. The radiation efficiency of an acoustic radiator is commonly defined as

$$\sigma = \Pi/\Pi_0 = \Pi/\tfrac{1}{2}\rho_0 ab\langle\overline{v_n^2}\rangle,$$

where ρ_0 is the density of the acoustic medium and $\langle\overline{v_n^2}\rangle$ is the spatial mean square velocity.

The plate has dimensions of $0{\cdot}3 \times 0{\cdot}2 \times 0{\cdot}001$ m. The material properties of aluminum are as follows: Young's modulus 70×10^9 N/m^2, Poisson ratio 0·3, density 2700 kg/m^3. The results from the analytical approach of Wallace [18] are compared with the present results. The comparison reveals good agreement, as shown in Figure 2.

3.2. CONTROL OF SOUND FIELDS FROM CANTILEVERED ISOTROPIC PLATE: EFFECTS OF ANISOTROPY

The integrated structure of an aluminum host structure and PVDF materials, bonded on the top and the bottom surface of the plate, and has the lay-up of $[0_{p+}/45_{p+}/I/-45_{p+}/0_{p-}]$, in which I represents the isotropic material, the subscript p represents the PVDF material, and the + and − signs represent the pole direction of the PVDF material in the thickness direction. The PVDF pair bonded at 0° with positive pole at the top surface and at 0° with negative pole at the bottom surface produce bending moments due to the electric field applied in the thickness direction; and the PVDF pair skewly bonded at −45° at the top and at 45° at the bottom with positive pole can induce a torsional moment due to the electric field applied in the thickness direction. Therefore, these two actuators have different control effects on the vibration modes of the cantilevered plate.

The integrated plate is clamped along the side on which $x = a/2$ and are free on the other sides (see Figure 1). The material properties of aluminum are the same as mentioned in the above example and the material properties of PVDF film are shown in Table 1. The dimensions of this structure are $a = 0{\cdot}3$ m, $b = 0{\cdot}2$ m and $h = 0{\cdot}00144$ m. The harmonic

TABLE 1

Material properties of graphite/epoxy and PVDF film

Graphite/epoxy	PVDF film
$E_{11} = 181{\cdot}0$ GPa	$E = 2{\cdot}0$ GPa
$E_{22} = 10{\cdot}3$ GPa	$v = 0{\cdot}3$
$G_{12} = 7{\cdot}17$ GPa	$\rho = 1780$ kg/m^3
$G_{13} = 7{\cdot}17$ GPa	$d_{31} = 23{\cdot}0 \times 10^{-12}$ V/m
$G_{23} = 2{\cdot}87$ GPa	$d_{32} = 3{\cdot}0 \times 10^{-12}$ V/m
$v_{12} = 0{\cdot}28$	$t = 0{\cdot}11$ mm
$t = 0{\cdot}125$ mm	
$\rho = 1520$ kg/m^3	

point force at ($0{\cdot}15$, $-0{\cdot}1$), a free corner of the cantilevered plate, excites all of the vibration modes of plate structure. The natural frequencies and mode shapes are shown in Table 2. The uncontrolled and controlled responses of the sound power are shown in Figure 3.

When only the $[0_{p+}/0_{p-}]$ actuator is used, the sound power is effectively suppressed in the off-resonance frequency region. In the frequency region of resonance corresponding to bending vibration modes (the first, the third, and so on), the sound power is also suppressed, as shown in Figure 3(a), although the peaks cannot be removed due to the limited control input. However, this actuator is not able to reduce the sound power induced by the plate in the frequency region of resonance corresponding to the torsional vibration modes—the second, the fourth, and so on—since the actuator cannot produce the necessary twisting moment for controlling the torsional motion of structure. When only the $[45_{p+}/-45_{p+}]$ actuator is used, the sound power is not effectively reduced in almost all of the frequency region. However, in the frequency region of resonance corresponding to torsional vibration modes, the actuator is effective, for it can generate pure torsional moments due to its skewed lamination angle. With these observations, two actuators are

TABLE 2

Natural frequencies and mode shapes of cantilevered isotropic plate

Mode number	Natural frequency (Hz)	Mode shape*
1	8·58	1LB
2	28·59	1T
3	53·69	2LB
4	97·43	2T
5	134·28	1CB
6	157·56	3LB
7	202·37	3T
8	213·79	2CB
9	314·07	4B
10	338·94	3CB
11	354·00	4T
12	378·33	5T
13	443·94	4CB
14	509·72	5CB
15	541·54	5LB

* LB, longitudinal bending mode; T, torsional mode; CB, chord-wise bending mode.

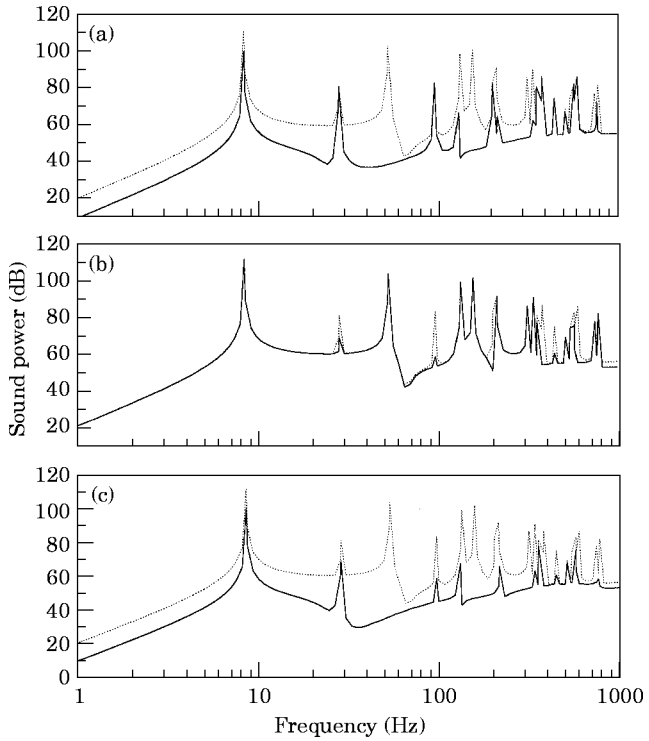

Figure 3. The sound power radiation from a simply supported integrated plate of $[0_{p+}/45_{p+}/0_l/-45_{p+}/0_{p-}]$. - - - -, Uncontrolled; ——, controlled with (a) only $[0_{p+}/0_{p-}]$ actuator, (b) only $[45_{p+}/-45_{p+}]$ actuator and (c) both $[0_{p+}/45_{p+}/-45_{p+}/0_{p-}]$ actuators.

used simultaneously, which results in the reduction of sound power radiation over the entire frequency region, as in Figure 3(c).

The anisotropic characteristic of PVDF actuators is utilized for the reduction of sound fields induced by bending and torsional vibrations of the structure. The results show that the anisotropy of PVDF actuators can improve the effectiveness of sound power control.

3.3. CONTROL OF RADIATED SOUNDS FIELDS FROM COMPOSITE PLATE: EFFECTS OF ANISOTROPY AND SHAPE

In this section, the composite plate and PVDF actuators with their own shapes and laminate angles are considered in order to investigate the influences of shape and anisotropy. The integrated plate is made of graphite/epoxy fiber reinforced composite materials and PVDF materials, bonded on both surfaces of the plate. The host structure is the laminated composite plate of $[0_c/\theta_c/-\theta_c/90_c]_s$, in which the subscript c represents the composite material. The material properties of the graphite/epoxy composite are shown in Table 1. The dimensions of host structure are $0{\cdot}3 \times 0{\cdot}2 \times 0{\cdot}001$ m. The harmonic point force is applied at $(0{\cdot}05625, 0{\cdot}06)$ in order to invoke all of the vibration modes of the composite plate.

The actuators used in this analysis are PVDF pairs, bonded with positive pole at the top surface and with negative pole at the bottom surface. The shapes of PVDF actuators considered here are depicted on the finite element mesh shown in Figure 4. The shaded area is the region of the actuator. The first one (Figure 4(a)) was used in the previous example of a cantilevered isotropic plate. The second actuator (Figure 4(b)) is denoted as

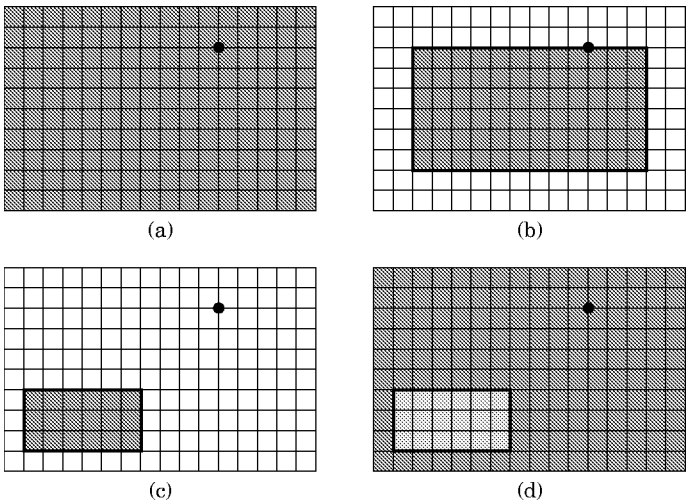

Figure 4. Four actuators used in control of the sound radiation from a composite plate: ● is the position of point force. (a) A1G; (b) A1C; (c) A1P; (d) A2M.

A1C and the third one (Figure 4(c)) is A1P. The lay-up angle of the PVDF actuator is represented by the subscript following the name of actuator; that is, $A1P_{\theta}$ denotes the actuator A1P with $[\theta_{p+}/\theta_{p-}]$ lay-up angles. The actuator, A2M, in Figure 4(d) consists of $A1P_{45}$ and the actuator covering the remaining surface area.

The control simulations for a simply supported composite plate are performed. The modal analysis results are presented in Table 3. First, actuator $A1C_0$ is used for the control of sound power. The result is shown in Figure 5. Actuator $A1C_0$ is effective for off-resonance frequencies and near-resonance frequencies related to odd vibration modes such as (1, 1), (3, 1) and (1, 3), but has no effect on near-resonance ranges about the even vibration modes. This actuator cannot control the even modes in an effective way since it is not coupled to those modes, due to its symmetrical shape with respect to x- and y-axes. Therefore it will be helpful to use another actuator with a non-symmetrical shape. Two

TABLE 3

Natural frequencies and mode shapes of a simply supported composite plate

Mode number	Natural frequency (Hz)	Mode shape
1	88·99	(1, 1)
2	213·14	(2, 1)
3	242·14	(1, 2)
4	359·54	(2, 2)
5	438·59	(3, 1)
6	519·38	(1, 3)
7	568·56	(3, 2)
8	647·70	(2, 3)
9	764·89	(4, 1)
10	826·52	(3, 3)
11	921·79	(4, 2)
12	974·10	(1, 4)
13	1094·82	(2, 4)
14	1138·85	(4, 3)
15	1218·36	(5, 1)

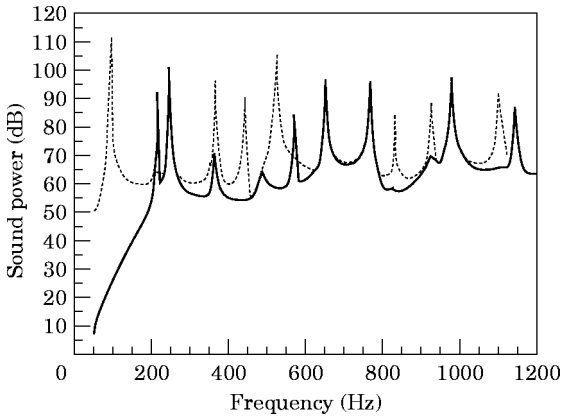

Figure 5. The sound power radiation from a simply supported integrated plate of $[0_p/0_c/45_c/-45_c/90_c]_s$. - - - -, Uncontrolled; ——, controlled with actuator $A1C_0$.

actuators have been tested for the same composite plate—one is $A1P_0$ and the other is $A1P_{45}$. These two actuators differ in their actuating moments. From equation (5), the actuating moments due to $A1P_0$ and $A1P_{45}$ are expressed as follows:

$$\begin{Bmatrix} \bar{M}_{xx} \\ \bar{M}_{yy} \\ \bar{M}_{xy} \end{Bmatrix}_{A1P_0} \propto \begin{Bmatrix} C_{11}d_{31} + C_{12}d_{32} \\ C_{12}d_{31} + C_{11}d_{32} \\ 0 \end{Bmatrix}, \qquad \begin{Bmatrix} \bar{M}_{xx} \\ \bar{M}_{yy} \\ \bar{M}_{xy} \end{Bmatrix}_{A1P_{45}} \propto \begin{Bmatrix} (C_{11} + C_{12})(d_{31} + d_{32}) \\ (C_{11} + C_{12})(d_{31} + d_{32}) \\ (C_{11} - C_{12})(d_{31} - d_{32}) \end{Bmatrix}.$$

Thus actuator $A1P_0$ can actuate bending moments only in the x and y directions, while $A1P_{45}$ can actuate not only bending moments in the x and y directions but also twisting moments.

Two actuators represent similarly good effectiveness for most frequencies, as shown in Figure 6. However, actuator $A1P_{45}$ is more effective in the sense that it can control more vibration modes than $A1P_0$, for example, the 12th mode. In order to compare the control

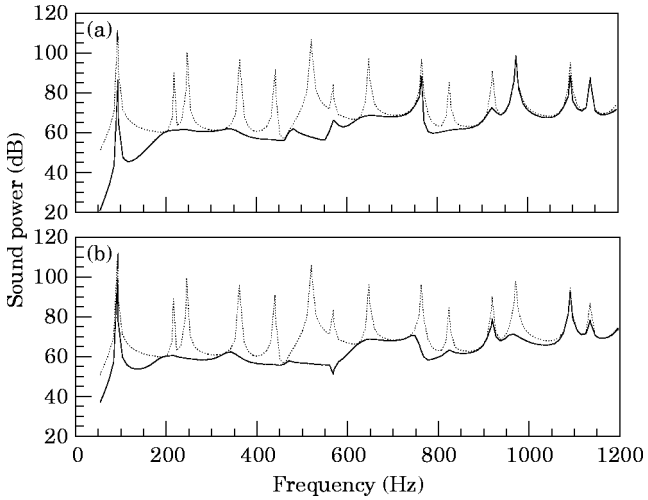

Figure 6. The sound power radiation from a simply supported integrated plate of $[0_p/0_c/45_c/-45_c/90_c]_s$. - - - -, Uncontrolled; ——, controlled (a) with actuator $A1P_0$ and (b) with actuator $A1P_{45}$.

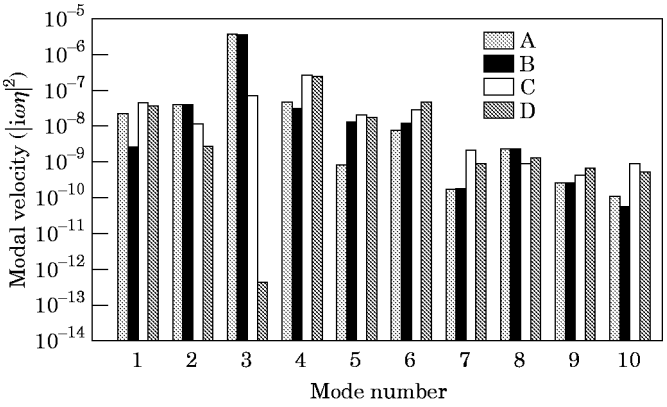

Figure 7. The modal velocity components of a simply supported integrated plate of $[0_p/0_c/45_c/-45_c/90_c]_s$ at 260 Hz. A, uncontrolled; B, controlled with actuator $A1C_0$; C, controlled with actuator $A1P_0$; D, controlled with actuator $A1P_{45}$.

effectiveness of actuators, the square modal velocity components are plotted at 260 Hz, close to the natural frequency of the third mode, (1, 2), in Figure 7. At this frequency, the response of the (1, 2) mode is dominant before control. After control, the third modal velocity is reduced when actuators $A1P_0$ and $A1P_{45}$ are used, but is not changed with actuator $A1C_0$; and the reduced value is the smallest in the case of actuator $A1P_{45}$.

Actuators $A1P_0$ and $A1P_{45}$ are effective over most of the frequency range, but they do not bring about notable reduction of the sound radiation from the resonance of the (1, 1) mode because their control force is not sufficient, due to the control input constraint. Actuator $A1C_0$ is efficient at the near-resonance of the (1, 1) mode. Therefore, actuator A2M is designed by adopting these advantages of $A1P_{45}$ and $A1C_0$. When actuator A2M is used, the sound radiation in the overall frequency regions can be attenuated effectively, as shown in Figure 8.

The same composite plate with a clamped boundary condition is also analyzed. With actuators $A1P_0$ and $A1P_{45}$, the radiated sound power is calculated in the frequency domain before and after control. The results in Figure 9 reveal that $A1P_0$ is more effective than $A1P_{45}$ for a clamped boundary condition, which is a different result from the case of the simply supported plate. It can be deduced that the actuator designed by the combination

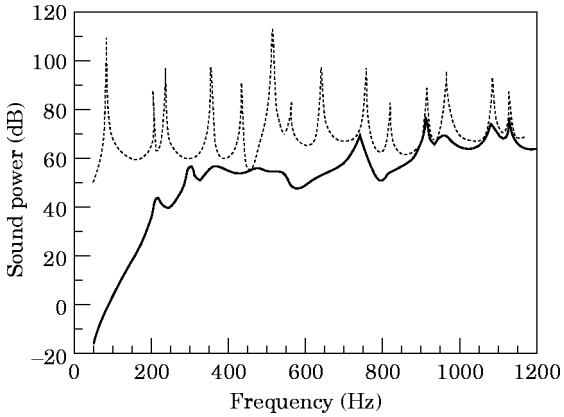

Figure 8. The sound power radiation from a simply supported integrated plate of $[0_p/0_c/45_c/-45_c/90_c]_s$. - - - -, Uncontrolled; ——, controlled with actuator A2M.

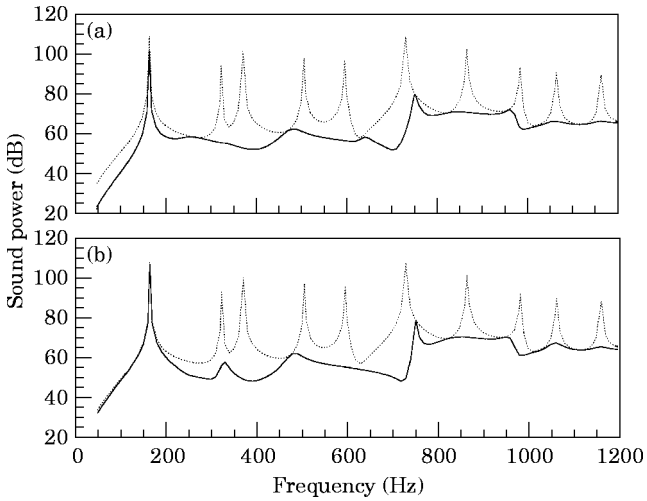

Figure 9. The sound power radiation from a clamped integrated plate of $[0_p/0_c/45_c/-45_c/90_c]_s$. - - - -, Uncontrolled; ——, controlled (a) with actuator $A1P_0$ and (b) with actuator $A1P_{45}$.

of $A1P_0$ and $A1C_0$ will show good effectiveness in the control of sound radiation from a clamped composite plate.

4. CONCLUSIONS

By using the anisotropic features and shapes of distributed polyvinylidene fluoride (PVDF) actuator, numerical investigations on the control of sound fields from a composite plate excited by a steady state point force were studied. The sound fields induced by the complicated dynamic behavior of the composite plate can be efficiently calculated with the coupled FEM–BEM code. For the cantilevered isotropic plate, the actuator, which is attached to produce the bending moment only, cannot reduce the radiated sound fields at near-resonance frequencies of torsional vibration modes. By combining this actuator with the actuator that has a skewed lamination angle, which can produce twisting moments, the effective reduction of sound radiation in the overall frequency range was obtained. The results show that the anisotropic characteristics of PVDF can be utilized as an efficient means of active control of structurally radiated sound fields. In the case of a simply supported composite plate, some distributed actuators with various shapes and ply angles are considered. The shape of the distributed actuator proved to be highly coupled to the vibration modes of the composite plates. It is possible to take advantage of the features to improve the effectiveness in acoustic noise control. Furthermore, the effects due to coupling between vibration modes and distributed PVDF actuator could be made better, without increasing the number of actuators, by changing the lamination angle of the actuator with the determined shape. The results obtained so far indicate that the anisotropy and the shape of the distributed piezopolymer suggest promising means for the design of more efficient actuators for controlling acoustic radiation from structures.

REFERENCES

1. C. R. FULLER 1990 *Journal of Sound and Vibration* **136**, 1–15. Active control of sound transmission/radiation from elastic plates by vibration inputs: I. analysis.

2. V. L. Metcalf, C. R. Fuller, R. J. Silcox and D. E. Brown 1992 *Journal of Sound and Vibration* **153**, 387–402. Active control of sound transmission/radiation from elastic plates by vibration inputs, I: experiments.
3. C. S. Pates III, U. S. Shirahatti and C. Mei 1995 *Journal of the Acoustical Society of America* **98**, 1216–1221. Sound–structure interaction analysis of composite panels using coupled boundary and finite element methods.
4. T. L. Turner, M. P. Singh and C. Mei 1995 *American Institute of Aeronautics and Astronautics Paper* 95-1303-CP. A spectral analysis approach for acoustic radiation from composite panels.
5. J. Y. Yu, W. Y. Kang and S. J. Kim 1995 *Journal of Composite Materials* **29**, 1201–1221. Elastic tailoring of laminated composite plate by anisotropic piezoelectric polymers—theory, computation, and experiment.
6. C. R. Fuller, C. H. Hansen and S. D. Snyder 1991 *Journal of Sound and Vibration* **150**, 179–190. Experiments on active control of sound radiation from a panel using a piezoelectric actuator.
7. R. L. Clark and C. R. Fuller 1992 *Journal of the Acoustical Society of America* **91**, 3313–3320. Experiments on active control of structurally radiated sound using multiple piezoelectric actuators.
8. S. Koshigoe, J. T. Gillis and E. T. Falangas 1993 *Journal of the Acoustical Society of America* **94**, 900–907. A new approach for active control of sound transmission through an elastic plate backed by a rectangular cavity.
9. R. L. Clark and C. R. Fuller 1992 *Journal of the Acoustical Society of America* **91**, 3321–3329. Modal sensing of efficient acoustic radiators with polyvinylidene fluoride distributed sensors in active structural acoustic control approaches.
10. R. L. Clark, R. A. Burdisso and C. R. Fuller 1993 *Journal of Intelligent Material Systems and Structures* **4**, 354–365. Design approaches for shaping polyvinylidene fluoride sensors in active structural acoustic control (ASAC).
11. K. Chandrashekhara and A. N. Agarwal 1993 *Journal of Intelligent Material Systems and Structures*, **4**, 496–508. Active vibration control of laminated composite plates using piezoelectric devices: a finite element approach.
12. O. O. Ochoa and J. N. Reddy 1992 *Finite Element Analysis of Composite Laminates*. Dordrecht, The Netherlands: Kluwer Academic.
13. C. K. Lee 1990 *Journal of the Acoustical Society of America* **87**, 1144–1158. Theory of laminated plates for the design of distributed sensors/actuators, part I: governing equations and reciprocal relationships.
14. D. T. Greenwood 1977 *Classical Dynamics*. Englewood Cliffs, NJ: Prentice-Hall.
15. K. J. Bathe and E. N. Dvorkin 1986 *International Journal for Numerical Methods in Engineering* **21**, 697–722. A four-node plate bending element based on Mindlin/Reissner plate theory and mixed formulations.
16. M. C. Junger and D. Feit 1986 *Sound*, *Structure*, *and Their Interaction*. Cambridge, MA: The MIT Press.
17. W. S. Hall 1993 *The Boundary Element Method*. Boston: Kluwer Academic.
18. C. E. Wallace 1972 *Journal of the Acoustical Society of America* **51**, 946–952. Radiation resistance of a rectangular panel.